Journal of Theoretical Biology 309 (2012) 113–120

Contents lists available at SciVerse ScienceDirect

Journal of Theoretical Biology

journal homepage: www.elsevier.com/locate/yjtbi

Density-dependent dispersal and population aggregation patterns

Vicenç Méndez [a,*], Daniel Campos [a], Ignacio Pagonabarraga [b], Sergei Fedotov [c]

[a] Grup de Física Estadística, Departament de Física, Universitat Autònoma de Barcelona, 08193 Bellaterra, Barcelona, Spain
[b] Departament de Física Fonamental, Facultat de Física, Universitat de Barcelona, Martí Franquès 1, 08028 Barcelona, Spain
[c] School of Mathematics, The University of Manchester, Oxford Road, Manchester M13 9PL, UK

HIGHLIGHTS

- We get conditions for the onset of spatial instability in reaction–dispersal–aggregation models.
- Our analytical predictions are tested to numerical simulations.
- We provide a stochastic interpretation of the non-linear aggregation terms.
- Long-dispersal is more stabilizing than diffusion.

ARTICLE INFO

Article history:
Received 12 December 2011
Received in revised form
7 June 2012
Accepted 12 June 2012
Available online 19 June 2012

Keywords:
Aggregation
Dispersal kernel
Spatial instability

ABSTRACT

We have derived reaction–dispersal–aggregation equations from Markovian reaction-random walks with density-dependent jump rate or density-dependent dispersal kernels. From the corresponding diffusion limit we recover well-known reaction–diffusion–aggregation and reaction–diffusion–advection–aggregation equations. It is found that the ratio between the reaction and jump rates controls the onset of spatial patterns. We have analyzed the qualitative properties of the emerging spatial patterns. We have compared the conditions for the possibility of spatial instabilities for reaction–dispersal and reaction–diffusion processes with aggregation and have found that dispersal process is more stabilizing than diffusion. We have obtained a general threshold value for dispersal stability and have analyzed specific examples of biological interest.

1. Introduction

It is known and well documented on the literature that individuals of a population can aggregate (Okubo, 1986). Actually, it is hard to find animals in nature that do not aggregate for one reason or another. Aggregations of motile animals can result from several distinct mechanisms classified by whether or not the motion of individuals is influenced by the presence of other individuals. If the motion is not influenced by neighbors, the motion is said to be density-independent, and it is said to be density-dependent if it is affected by the presence of other individuals. The gregarious behavior can be motivated by the need for survival, reproduction or to overcome a hostile environment. This behavior can also increase the chance of avoiding capture by a predator. As a result, individuals can undergo two different motions: attraction or repulsion. Attraction between individuals of the same species can occur either through indirect (different taxis mechanisms such as chemotaxis, phototaxis, etc.) or direct attraction. In this latter case, individuals attract conspecifics due to social interactions (mating, settlement, etc.) or to defense against predators (Fedotov et al., 2008). However, it is the lower resources in the highly populated regions which causes exodus, i.e., a repulsive movement due to aggregation. The population pressure forces the individuals to move away from regions of large population densities. The existence of a critical population density which separates attractive from repulsive phenotypic response was considered by Turchin (1989).

There exist several theoretical models that account for aggregation. Some of them deal with indirect attraction and require two partial differential equations (PDEs) to account both for (i) the evolution of the population density and (ii) the balance equation for the attractive substance. This is the so-called chemotaxis–reaction–diffusion scenario (Murray, 2003). Others only involve one PDE for the individuals motion but are nonlinear due to aggregation. The most common equation, known as density-dependent Fisher equation or density-dependent reaction–diffusion equation, constitutes a simple extension of the Fisher equation with a diffusion coefficient that depends explicitly on the population density (Murray, 2003). This equation can be obtained by combining the balance equation for the population

* Corresponding author. Tel.: +34 3 5812575.
E-mail address: vicenc.mendez@uab.es (V. Méndez).

0022-5193/$ - see front matter © 2012 Elsevier Ltd. All rights reserved.
http://dx.doi.org/10.1016/j.jtbi.2012.06.015

density with a Fick's law for the individual's flux where the diffusion coefficient depends on the density. This equation was derived by Turchin (1989) from a random walk model on a lattice with constant spacing and assuming that the probabilities of jumping to the right or left are not constant. The merit of this derivation is to connect the diffusion coefficient with microscopic features of the underlying random walk such as the bias due to the presence of other individuals. This helps to understand the origin of aggregation in the density-dependent reaction–diffusion models. However, most models are phenomenological and introduce *ad hoc* non-linear or non-local terms such as nonlinear advection. There are several works that consider the diffusion coefficient as a linearly increasing function of the density (Gurney and Nisbet, 1975; Shigesada et al., 1979; Petrovskii and Li, 2003; Almeida et al., 2006; Balasuriya and Gottwald, 2010; Kenkre and Kumar, 2008), other models involve nonlinear dependences (Turchin, 1989; Smith et al., 2008; Maini et al., 2006; Sánchez-Garduño et al., 2010; Cates et al., 2010). Most of those works study the conditions for the existence and uniqueness of traveling wave solution (front propagation) or the emergence of spatial instabilities due to nonlinear couplings. Other models incorporate nonlinear advection terms in addition to the density-dependent diffusion coefficient (Okubo, 1986). These terms are also present in models for chemotaxis. There are models with nonlocal advection terms to deal with long distance attraction described through a spatial kernel (Grünbaum and Okubo, 1994) and have been applied to model cell–cell adhesion (Armstrong et al., 2006). Another line of research consists of identifying aggregation with nonlocal competition (Britton, 1989). Only the works by Okubo (1986), Turchin (1989) and more recently Petrovskii and Li (2003), have made an effort to connect the density-dependent reaction–diffusion models with the microscopic details of the random motion. More recently, Fedotov (2011) has derived a model from residence time structured model to study the emergence of anomalous aggregation due to crowding effects.

Moreover, it is well known that the displacement of many animals can be properly described by random walks (Othmer et al., 1988; Okubo and Kareiva, 2001). The distance that individuals travel can be described as random draws from a probability density function termed a dispersal kernel. These kernels have been measured for a tremendous number of organisms (Kot et al., 1996). This can have important effects in the spatial dynamics of biological systems. For example, the invasion rate obtained from the classical reaction–diffusion equation (Skellam, 1951) cannot predict, for example, fast plant migration (Reid's paradox) since reaction–diffusion always underestimates the observed value. The paradox was solved by describing the movement using dispersal kernels with fat tails (Clark, 1998).

Besides the importance of dispersal in ecology there is a growing realization of the influence of density-dependence in movement rate as well. Density-dependent dispersal in demographic processes is crucial to the study of population dynamics (Matthysen, 2005). Increasingly, density-dependent dispersal kernels are being implemented in both theoretical and applied population models (e.g. Wu et al., 1993; Veit and Lewis, 1996; Ims and Andreassen, 2005). Furthermore, it has been experimentally observed that density-dependent dispersal leads to aggregation population patterns (de Jager et al., 2011; Igoshin et al., 2001, 2004).

The aim of this work is twofold. First of all we want to give a wide, and at the same time simple, stochastic foundation to aggregation due to the presence of conspecifics. We shall consider a Markovian random walk with density-dependent jump rate or density-dependent biased jumps with a general dispersal kernel. In both cases we take the diffusion limit to derive the corresponding macroscopic density-dependent reaction–diffusion equations. As particular cases, we shall recover well-known equations and provide an expression for the density-dependent diffusion coefficient in terms of the second moment of the dispersal kernel and the nonlinear advection term. On the other hand, we shall show how our model can predict patterns of population aggregation by considering density-dependent dispersal kernels, providing a microscopic explanation. To this end, we study the role of the dispersal kernel (in comparison with the diffusion approach) in the emergence of spatial instabilities both considering density-dependent jump rate (observed experimentally by Ims and Andreassen, 2005; Igoshin et al., 2001, 2004) and density-dependent dispersal kernels in one dimension (observed very recently by de Jager et al., 2011). In both cases we show that the conditions for the emergence of spatial diffusive-instability are less restrictive than for spatial dispersal-instability. This means the dispersal processes have a stronger stabilizing effect than diffusion. In particular, we show the existence of a threshold value for the quotient between the reaction and jump rates above which it is not possible a spatial dispersal instability.

2. Stochastic foundation of reaction–diffusion–aggregation

Let $X(t)$ be the position of a particle at time t. If jumps are Markovian the probability of a jump during the small time interval $(t,t+\Delta t]$ is $\lambda[X(t)]\Delta t+O(\Delta t^2)$, so that $X(t+\Delta t)=X(t)+Z(t)+O(\Delta t^2)$ with $Z(t)$ the jump distance. The conditional density for a stationary jump process $Z(t)$ is the dispersal kernel

$$\Phi(z)=\frac{\partial}{\partial z}\mathbb{P}\{Z(t)\le z\}$$

and the balance of particles at point x

$$\rho(x,t+\Delta t)=\Delta t\int_{\mathbb{R}}\lambda\rho(x-z,t)\Phi(z)\,dz+(1-\lambda\Delta t)\rho(x,t)+O(\Delta t^2). \tag{1}$$

Subtracting $\rho(x,t)$ from both sides, dividing by Δt and letting $\Delta t\to 0$ we obtain the mesoscopic equation

$$\frac{\partial\rho}{\partial t}=\int_{\mathbb{R}}\lambda\rho(x-z,t)\Phi(z)\,dz-\lambda\rho(x,t). \tag{2}$$

Since the jump process is Markovian it is easy to account for population growth simply by adding a reaction function $F(\rho)$ to the right hand side of (2). In non-Markovian models $\rho(x,t)$ depends on the probability that particles reached the point x at time a previous time, say $t-\tau$. However, if mortality effects are considered then those particles that reached the position x at $t-\tau$ may have died and this should be taken into account in the transport term of the equations. For this reason, it is indispensable to couple transport and reaction in non-Markovian models and the reaction term cannot be simply added to the transport equation (Méndez et al., 2010). If we want to consider overcrowding effects such us aggregation then we can assume that the jump rate λ depends explicitly on ρ

$$\frac{\partial\rho}{\partial t}=\int_{\mathbb{R}}\lambda[\rho(x-z,t)]\rho(x-z,t)\Phi(z)\,dz-\lambda[\rho(x,t)]\rho(x,t)+F(\rho) \tag{3}$$

or, alternatively, the dispersal kernel depends explicitly on ρ

$$\frac{\partial\rho}{\partial t}=\lambda\int_{\mathbb{R}}\rho(x-z,t)\Phi[z,\rho(x-z,t)]\,dz-\lambda\rho(x,t)+F(\rho). \tag{4}$$

Since Eqs. (3) and (4) contain a dispersal kernel instead of spatial derivatives they account for a rather general spread mechanism than diffusion. Likewise, due to the density dependence of the jump rate or the dispersal kernel and the presence of a reaction term, they constitute a generalization of the classical and well-known reaction–diffusion–aggregation equations.

3. The diffusion limit

In this section we analyze the diffusion regime of the evolution equations obtained in Eqs. (3) and (4)

3.1. Density-dependent jump rate

Density-dependent jump rates have been observed in microorganisms such myxobacteria cells (Igoshin et al., 2001) and tundra vole (Ims and Andreassen, 2005). In both cases the jump rate depends nonlinearly with the density. To perform the diffusion limit we consider the jump distance small compared to the spatial scale x so that

$$\rho(x-z,t) \simeq \rho(x,t) - \frac{\partial \rho}{\partial x} z + \frac{1}{2}\frac{\partial^2 \rho}{\partial x^2} z^2 + O(z^3) \tag{5}$$

and

$$\lambda[\rho(x-z,t)]\rho(x-z,t) = \rho\lambda(\rho) - z\frac{\partial}{\partial x}[\rho\lambda(\rho)] + z^2\frac{1}{2}\frac{\partial^2}{\partial x^2}[\rho\lambda(\rho)] + O(z^3). \tag{6}$$

Inserting (5) and (6) into (3), gathering terms and considering the statistical properties of the dispersal kernel

$$\int_{\mathbb{R}} \Phi(z)\, dz = 1, \quad \int_{\mathbb{R}} z\Phi(z)\, dz = 0, \quad m_2 = \int_{\mathbb{R}} z^2 \Phi(z)\, dz, \tag{7}$$

corresponding to isotropic random walks with finite moments, we have that (3) becomes

$$\frac{\partial \rho}{\partial t} = \frac{m_2}{2}\frac{\partial^2}{\partial x^2}[\rho\lambda(\rho)] + F(\rho), \tag{8}$$

or equivalently

$$\frac{\partial \rho}{\partial t} = \frac{\partial}{\partial x}\left[D(\rho)\frac{\partial \rho}{\partial x}\right] + F(\rho), \tag{9}$$

where

$$D(\rho) = \frac{m_2}{2}\frac{d}{d\rho}[\rho\lambda(\rho)]. \tag{10}$$

Note that $D(\rho)$ plays the role of effective density-dependent diffusion coefficient. This has been widely employed in theoretical ecology to model population aggregation. Eq. (9) is known as the density-dependent Fisher equation and has been widely studied (see for example: Turchin, 1989; Murray, 2003). With this derivation we give a clear and simple microscopic interpretation to the $D(\rho)$. Eq. (10) shows the dependence of the diffusion coefficient on the density-dependent jump rate. Other mesoscopic interpretations have been done by Okubo (1986) and Turchin (1989) extending the idea of random walk in a lattice with density-dependent probabilities to jump to the right or to the left. For example, Eq. (8) was derived by Turchin (1989), where $\rho\lambda(\rho)$ was related to jump probabilities of jumping to right or left in a lattice of fixed spacing. In this work we provide a more general framework to explain aggregation which is at the same time simple and easily connected to the underlying microscopic features.

In the context of bacterial colony evolution, Cates et al. (2010) have recently observed aggregation patterns of *E. coli* by considering a run-and-tumble motion with density-dependent speed. Their model resembles very much the one obtained in (9). In this system the diffusive behavior of the bacteria colonies can be understood from the dependence of run and tumbling events of the individual microorganisms on their environment (Tailleur and Cates, 2008). Thompson et al. (2011) have analyzed how such effective diffusion coefficient can be understood from microscopic, lattice-based, models for population dynamics.

3.2. Diffusion limit for density-dependent dispersal kernel

Density-dependent dispersal kernels have been recently found in the dispersal of mussels (de Jager et al., 2011). Although the dispersal distances are unaffected by mussel density the authors find that the probability of movement depends on ρ. Then, it suggests to consider the form $\Phi[z,\rho(x-z,t)]$. Expanding $\Phi[z,\rho(x-z,t)]$ for $z \ll x$ we get

$$\Phi[z,\rho(x-z,t)] \simeq \Phi(z,\rho) + \frac{\partial \Phi}{\partial \rho}\left[-z\frac{\partial \rho}{\partial x} + \frac{1}{2}\frac{\partial^2 \rho}{\partial x^2} z^2\right] + \frac{1}{2}\frac{\partial^2 \Phi}{\partial \rho^2} z^2 \left(\frac{\partial \rho}{\partial x}\right)^2 + O(z^3). \tag{11}$$

Inserting (5) and (11) into (4) one finds, after considering the properties (7), exactly the same equation (9) but now

$$D(\rho) = \frac{\lambda}{2}\frac{d}{d\rho}[\rho m_2(\rho)] \quad \text{with } m_2(\rho) = \int_{\mathbb{R}} z^2 \Phi(z,\rho)\, dz. \tag{12}$$

In summary, we have given two different microscopic foundations to the well-known reaction–diffusion–aggregation equation (9) and have shown different origins which can lead to effective density-dependent diffusion coefficients.

3.3. Diffusion limit for biased dispersal

Let us consider that there exists an "aggregation force" that modifies the isotropy of the dispersal process by introducing some bias, i.e. $\int_{\mathbb{R}} z\Phi(z)\, dz \neq 0$. The diffusion limit corresponding to the case of density-dependent jump rate contains now two additional terms in such a way that the final PDE has a new nonlinear advection term

$$\frac{\partial \rho}{\partial t} = \frac{\partial}{\partial x}\left[D(\rho)\frac{\partial \rho}{\partial x}\right] - \chi(\rho)\frac{\partial \rho}{\partial x} + F(\rho), \tag{13}$$

where

$$\chi(\rho) = m_1 \frac{d}{d\rho}[\rho\lambda(\rho)] \quad \text{with } m_1 = \int_{\mathbb{R}} z\Phi(z)\, dz.$$

For the case of density-dependent dispersal kernel the final equation reads as (13) but now

$$\chi(\rho) = \frac{d}{d\rho}[\rho m_1(\rho)] \quad \text{with } m_1(\rho) = \int_{\mathbb{R}} z\Phi(z,\rho)\, dz.$$

4. Spatial instabilities

In this section we study the emergence of spatial instabilities in one-dimensional one-component reaction–diffusion and reaction–dispersal equations with aggregation. It is well known that the one-dimensional Fisher equation (Eq. (9) with $D(\rho) = \text{constant}$) is not able to describe spatial instabilities (Murray, 2003) and at least a two-component systems with activator–inhibitor dynamics is required. However, we show here that the model introduced in the previous section can exhibit spatial patterns due to aggregation. To this end, we exploit the fact that both Eqs. (3) and (4) admit a homogeneous population steady state, ρ_0, corresponding to the zeros of the reaction term, $F(\rho_0) \equiv F_0 = 0$. These homogeneous states are stable if $F'(\rho_0) < 0$, where the prime refers to the derivative of the function with respect to the function argument. To analyze the growth of spatial instabilities we perform a standard linear stability analysis about the homogeneous steady state ρ_0. Specifically, we let $\rho(x,t) = \rho_0 + \delta\rho(x,t)$ where $\delta\rho(x,t)$ is a small perturbation. We will analyze separately the situations where the jump rate and the dispersal kernel depend on the population density.

4.1. Density-dependent jump rate

Substituting the previous expression for density variations in Eq. (3) and neglecting nonlinear terms in $\delta\rho(x,t)$, the linear evolution equation for the perturbations in the case of density-dependent jump rate is

$$\frac{\partial\delta\rho}{\partial t}=D(\rho_0)\left[\int_{\mathbb{R}}\delta\rho(x-z,t)\Phi(z)\,dz-\delta\rho(x,t)\right]+F'(\rho_0)\delta\rho(x,t), \tag{14}$$

where we have considered (10).

Introducing spatiotemporal variations of the form $\delta\rho(x,t)=\delta\tilde{\rho}\,e^{ikx+\mu t}$ into Eq. (14), where k and μ stand for the wave number and the growth rate, respectively, yields the dispersion relation

$$\mu\delta\tilde{\rho}=\left\{\frac{2}{m_2}\tilde{D}_0[\hat{\Phi}(k)-1]+F_0'\right\}\delta\tilde{\rho}. \tag{15}$$

where $\hat{\Phi}(k)$ corresponds to the Fourier transform of the dispersal kernel and $\tilde{D}_0=2D(\rho_0)/m_2$ stands for the value of the effective density in the reference, homogeneous state. The dispersion relation (15) that controls the instability of the homogeneous state can be expressed as

$$\mu=-\tilde{D}_0\hat{\psi}(k)+F_0', \tag{16}$$

where $F_0'\equiv F'(\rho_0)$ and for simplicity's sake, we account for the k-dependence of the dispersal kernel through

$$\hat{\psi}(k)\equiv\frac{2[1-\hat{\Phi}(k)]}{m_2},$$

which in the diffusion limit reduces to $\hat{\psi}(k)\simeq k^2+O(k^4)$. Since homogeneous configurations are stable to homogeneous perturbations, $F_0'\leq 0$, for diffusive dispersal models the necessary condition for their instability is that the corresponding effective diffusion is negative, $\tilde{D}_0<0$. It is clear, from the motivation of the dispersal models, that we have to ensure that jumps are positive, hence $\lambda(\rho)>0$. However, this restriction is compatible with a negative effective diffusion coefficient. This is achieved for sufficiently fast logarithmic variations of the jump rate, i.e. $d\ln\rho/d\ln\lambda\leq -1$ (this condition is obtained by requiring $D(\rho)<0$ in Eq. (10)). The sufficient condition for pattern formation can be then expressed as

$$\hat{\psi}(k)\geq\frac{|F_0'|}{\tilde{D}_0}, \tag{17}$$

if $\hat{\psi}(k)\geq 0$. As we will discuss below, this is the case for a wide family of usual dispersal kernels. Under this condition, we can see that once the effective diffusion becomes negative, the homogeneous state is necessarily unstable and will develop spatial patterns. This instability is independent of the reaction rate. The competition between jump kinetics and population growth and death will determine the range of wave lengths which become unstable, hence being relevant to determine the characteristic time scales associated to the development of the corresponding patterns. Since in the diffusion regime $\hat{\psi}(k)\simeq k^2$, the higher the wave number the higher the growth rate. The instability will therefore develop from very small scales. The lowest unstable mode in the diffusive regime corresponds to $k_{\min}=\sqrt{|F_0'|/|\tilde{D}_0|}$.

The conditional jump rate determines also a bound for $\hat{\Phi}(k)$. Accordingly, the diffusive regime becomes incorrect at large wave vectors. The finite bound of $\hat{\Phi}(k)$ implies that asymptotically $\hat{\psi}(k)\to 2/m_2$ for $k\to\infty$. As a result, the restriction in particle jumps introduces a dispersal-stabilization mechanism that can counterbalance the short scale instability induced by the negative effective diffusion coefficient. Quantitatively, dispersion stabilizes the homogeneous density configuration if

$$\frac{2|\tilde{D}_0|}{m_2|F_0'|}\leq 1, \tag{18}$$

which depends on the competition between diffusion and dispersal rate through the second moment of the conditional jump rate.

Therefore, we can identify a finite window where the (low) density-dependence of the dispersal is not relevant when the homogeneous configuration becomes stable. If the state is unstable, the destabilization mechanism is always controlled by short scale fluxes due to the effective negative density. In this respect, the expected spatial patterns will be characterized by generic features for any dispersal kernels. The negative effective diffusion coefficient indicates that as particles move from low to high density regions, their effective motility is reduced in the later regimes. At the same time, in these large density regimes particles tend to die more easily (because of the stability properties of the reference state ρ_0 as dictated by the corresponding reaction rate $F(\rho)$). As a result, large density domains of small spatial extent develop and end up being sustained by the net flux of incoming particles from lower density regions, where the positive reaction rate provides a continuous supply of particles. Due to the generality of the instability mechanism, we expect that patterns are analogous to those reported for bacterial colonies with a motility reduced at higher bacterial concentrations (Cates et al., 2010) and will be formed by relatively isotropic and static islands of large (small) density aggregates of particles in a background of small (large) particle density depending on the system parameters.

Although the basic mechanism controlling the growth of the small domains is independent of the structure of the dispersal kernel, the relative weight of the unstable wave vectors varies. As a result, since the instability is controlled by the higher wave vectors and their distribution depends on the dispersal kernel, there may be a weak dependence of the formed domains on the structure of the dispersal kernel. Quantitatively, if $m_2|F_0'|/|\tilde{D}_0|>1$, all unstable modes will grow slower than predicted in the diffusive limit. Moreover, the larger the wave vector the closer the corresponding growth rates. Therefore, the dispersal nature of the kernel will become apparent both because the development of the unstable structures will be slower than expected on the basis of the corresponding diffusive limit and because there will be more marked mode mixing (i.e. a wider instability band of unstable modes).

4.1.1. Examples

To analyze specifically how dispersal can lead to inhomogeneous aggregation, we consider the particular dependence

$$\lambda(\rho)=(1-\alpha\rho+\beta\rho^2)/\tau, \tag{19}$$

where α and β are two positive parameters. This is equivalent to the density-dependent diffusion coefficient considered by Turchin (1989) for *A. varians*. This dependence takes into account that the jump rate will decrease initially as ρ increases due to crowding effects (aggregation). However, at high densities ($\rho>\alpha/2\beta$) the jump rate will increase as ρ increases since individuals continuously come into contact and induce each other to disperse (repulsion). A physical restriction on the parameters α and β comes from the fact that the jump rate has to be positive. To guarantee $\lambda(\rho)>0$, we shall require that the minimum value of $\lambda(\rho)$ is positive, so $\alpha^2<4\beta$. Alternatively, we could allow $\alpha^2>4\beta$ and the physical restriction $\lambda>0$ would require $\beta>\alpha-1$ but have checked that there are no qualitative differences. These restrictions are consistent with a negative diffusion coefficient. When the reaction term, which models population reproduction and death, follows the logistic equation, $F(\rho)=r\rho(1-\rho)$, according to

Eqs. (18) and (19), the homogeneous configuration becomes spatially unstable for

$$\hat{\psi}(k) > \frac{r\tau}{2\alpha-3\beta-1}, \tag{20}$$

assuming the necessary condition of a negative effective diffusion coefficient, $1-2\alpha+3\beta<0$. Therefore, for the dispersal driven instability to occur it is necessary that the equality in (20) has positive solution, i.e.,

$$2\alpha-3\beta-1 > r\tau, \tag{21}$$

assuming that $\hat{\Phi}(k)>0$ for all k. As pointed out earlier, the ratio between reaction and jump rates controls the possibility of developing spatial instabilities. If an instability is allowed, the minimal unstable mode, k_c, obeys

$$\hat{\Phi}(k_c) = 1-\frac{r\tau}{2\alpha-3\beta-1}. \tag{22}$$

In order to gain further insight into the features associated to dispersal controlled spatial instabilities, we will consider some specific dispersal kernels widely used in ecology (Kot et al., 1996). As a first example, the Gaussian kernel

$$\Phi(z) = \frac{1}{\sigma\sqrt{\pi}} e^{-z^2/\sigma^2},$$

leads to $\hat{\Phi}(k) = e^{-\sigma^2 k^2/4}$ and $m_2 = \sigma^2/2$. The dispersion relation, Eq. (15), reads

$$\mu = \frac{1}{\tau}(-2\alpha+3\beta+1)[e^{-\sigma^2k^2/4}-1]-r \tag{23}$$

and the band of unstable modes in this case reduces to

$$k^2 > k_c^2 = -\frac{4}{\sigma^2}\ln\left[1-\frac{r\tau}{2\alpha-3\beta-1}\right].$$

The second example is the Laplace dispersal kernel

$$\Phi(z) = \frac{1}{2\sigma} e^{-|z|/\sigma},$$

also widely used in dispersal ecology. In this case we have $\hat{\Phi}(k) = (1+\sigma^2k^2)^{-1}$ and $m_2 = 2\sigma^2$. From (15)

$$\mu = \frac{1}{\tau}(-2\alpha+3\beta+1)\left[\frac{1}{1+\sigma^2k^2}-1\right]-r \tag{24}$$

and

$$k^2 > k_c^2 = \frac{1}{\sigma^2}\frac{r\tau}{2\alpha-3\beta-1-r\tau}.$$

As we have shown in Eq. (21), in the regime where

$$0 < 2\alpha-3\beta-1 < r\tau, \tag{25}$$

there is diffusion instability but there is no dispersal instability. In this diffusion regime the dispersion relation reduces to

$$\mu = -\frac{k^2\sigma^2}{4}(1-2\alpha+3\beta)-r. \tag{26}$$

In Fig. 1 we display the different stable and unstable phases for the current dispersal model for the two positive kernels discussed.

We have compared different kernels with the same mean (zero) and variance (m_2) so that the difference is only for the kernel moments m_n with $n>2$, that vanish in the diffusion limit. In Fig. 2, we draw the corresponding phase diagrams as a function of α and β. We have labeled each region and the "non-physical region" corresponds to the domain where the jump rate is negative. In the right hand side panel $r\tau<1/3$ while in the left hand side panel $r\tau>1/3$ and the dispersal driven instability disappears (see the figure caption for details). This is a very interesting result, absent in the diffusion approach, that shows the importance of the ratio between reaction rate and jump rate on dispersal-driven instabilities.

In Fig. 2 we also show the results obtained from the numerical integration of Eq. (3) just to confirm that they properly match the

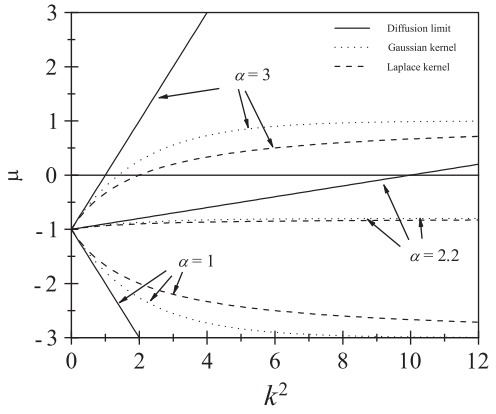

Fig. 1. Dispersion relations for diffusion limit (solid curves), Gaussian kernel (dotted curves) and Laplace kernel (dashed-dotted curves). It is observed three different situations where there is no spatial instability ($\alpha=1$), only the diffusion limit predicts instability ($\alpha=2.2$) and both diffusion and dispersal transport predict instability ($\alpha=3$). $\tau=\beta=r=m_2=1$.

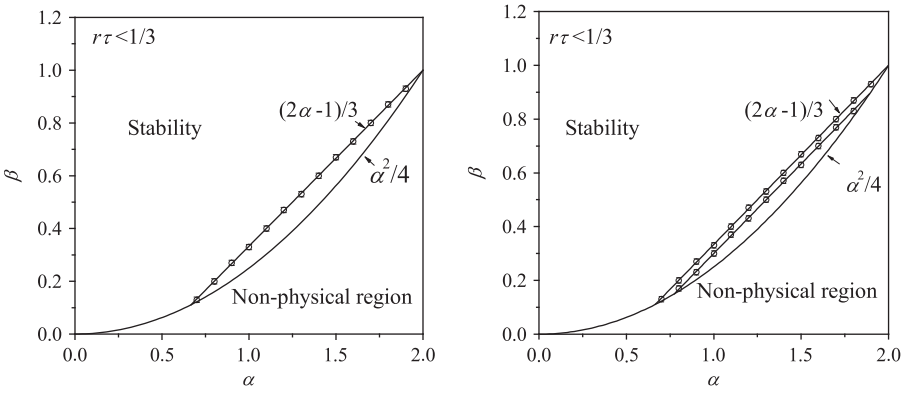

Fig. 2. Parameter space diagram for the regions of stability and instability obtained from conditions (25). Circles and the corresponding error bars correspond to the results obtained from the numerical integration of Eq. (3). The non-physical region is $\lambda(\rho)<0$. $r\tau=0.1$. Left panel: the region between the stability and non-physical domains corresponds to diffusion instability. The circles correspond to the numerical values for which the onset to diffusion instability is observed. In this panel $r\tau>1/3$ and dispersal is always stabilizing. Right panel: the region between the stability and non-physical domains but closer to the stability domain correspond to diffusion instability while the closer to the non-physical region corresponds to diffusion and dispersal instability.

different stability regions predicted by our theoretical derivations. To check this, we have integrated the equation up to a certain (large enough) time and have observed if the solution $\rho(x,t)$ tended asymptotically to the constant stable point $\rho=1$ or reached a non-homogeneous solution (i.e. a pattern) for different values of α and β. The corresponding results (circles) confirm that the agreement with the theory is excellent. In accordance to our discussion above, we observe that regions of instability are characterized by non-regular patterns of $\rho(x,t)$ as those observed in Cates et al. (2010) which become more irregular in the diffusion case (due to short-range dispersal, which makes the instability a more local phenomena) and much smoother when dispersal kernels are considered.

For heavy-tailed dispersal kernels, such as a Lévy dispersal kernel, one has $\hat{\Phi}(k)=e^{-a|z|^{\varsigma}}$ with $0<\varsigma<2$ (Méndez et al., 2010) which is also positive definite and hence will have a behavior analogous to the one studied for the widespread Gaussian and Laplace dispersal kernels. A different mechanism for pattern formation may in principle appear if the dispersal kernel is bounded. If we consider the top-hat kernel, $\Phi(z)=\Theta(\sigma-|z|)/(2\sigma)$, its Fourier transform oscillates as

$$\hat{\Phi}(k)=\frac{\sin k\sigma}{k\sigma}. \tag{27}$$

This kernel will develop regions where $\hat{\Phi}(k)$ is negative for some bands of modes. In these situations, the homogeneous density state can become unstable even if $\tilde{D}_0>0$, and the most unstable, growing mode, is characterized by the specific form of the dispersal kernel (σ in the previous, simple example). This is a different scenario to promote pattern formation as compared with the standard scenario put forward earlier, where instabilities develop always from the smallest scales. It is interesting to note that as σ becomes smaller, $\hat{\psi}(k)$ becomes negative at larger k values. Hence, asymptotically, for large σ this mechanism will not be distinguishable from the one associated to positive-definite dispersal kernels. In general, depending on the ratio $|F_0'|/|\tilde{D}_0|$ and the value of σ it is then possible to have different sources of instability depending on the sign of $\tilde{D}_0$.

4.2. Density-dependent dispersal kernel

It is possible to carry out an analogous study as performed in the previous subsection when the dispersal-kernel depends on the local density. Considering a small variation of the population density around the homogeneous steady configuration, ρ_0. Inserting $\rho(x,t)=\rho_0+\delta\rho(x,t)$ into (4) and linearizing one gets

$$\frac{\partial\delta\rho}{\partial t}=\lambda\left[\int_{\mathbb{R}}\delta\rho(x-z,t)\left\{\left[\frac{\partial\Phi(z,\rho)}{\partial\rho}\right]_{\rho=\rho_0}+\Phi(z,\rho_0)\right\}dz-\delta\rho(x,t)\right]+rF_0'\delta\rho.$$

The dispersal relation in this case can be expressed as

$$\mu=\lambda[\hat{\Phi}_{\rho}(k,\rho_0)+\hat{\Phi}(k,\rho_0)-1]+F_0', \tag{28}$$

where we have defined

$$\hat{\Phi}_{\rho}(k,\rho_0)=\mathcal{F}_z\left\{\left[\frac{\partial\Phi(z,\rho)}{\partial\rho}\right]_{\rho_0}\right\}$$

and

$$\mathcal{F}_z\{\Phi(z,\rho)\}=\int_{\mathbb{R}}e^{-ikz}\Phi(z,\rho)\,dz.$$

The condition for spatial instability now reads

$$\hat{\Phi}_{\rho}(k,1)+\hat{\Phi}(k,1)>1-\frac{F_0'}{\lambda}$$

and the equation for the band of unstable modes is

$$\hat{\Phi}_{\rho}(k_c,1)+\hat{\Phi}(k_c,1)=1-\frac{F_0'}{\lambda}.$$

Due to the dependence of the dispersal kernel on density, it is less obvious in this case to correlate the instability to the sign of an effective diffusion, or the fact that the dispersal kernel is positive-definite. Since the macroscopic limit in this case allows us to define an effective diffusion coefficient it is expected to obtain the same type of spatial patterns as for the case of density-dependent jump rate.

4.2.1. Examples

We can gain insight on the instability scenarios induced by a density-dependent dispersal kernel by analyzing first dispersal kernels with density-dependent variances. For the widely used Gaussian and Laplace kernels with equal variances one has

$$\Phi(z,\rho)=\frac{1}{\sqrt{2\pi m_2(\rho)}}e^{-z^2/2m_2(\rho)} \tag{29}$$

and

$$\Phi(z,\rho)=\frac{1}{\sqrt{2m_2(\rho)}}e^{-|z|\sqrt{2}/\sqrt{m_2(\rho)}}, \tag{30}$$

respectively. Using Eqs. (29) and (30), the corresponding dispersion relations for the logistic growth term, $F(\rho)$, can be derived as

$$\mu=\lambda\left[1-\frac{m_2'(1)k^2}{2}\right]e^{-m_2(1)k^2/2}-\lambda-r$$

and

$$\mu=\lambda\frac{1+\frac{k^2}{2}[m_2(1)-m_2'(1)]}{\left(1+\frac{m_2(1)k^2}{2}\right)^2}-\lambda-r$$

for the Gaussian and Laplace dispersal kernels, respectively.

Let us choose a monotonically decreasing variance, i.e., $m_2(\rho)=m_0\rho^{-n}$ with $n>0$. For the Gaussian kernel, the band of unstable spatial modes lies between the solutions of the equation $(1+ny^2)e^{-y^2}=1+r/\lambda$. This equation has solution if the maximum of $(1+ny^2)e^{-y^2}$ is higher than $1+r/\lambda$. There are two solutions if and only if $n>n_c$, where n_c is solution to $n_ce^{-1+1/n_c}=1+r/\lambda$. For the Laplace kernel this condition reads $n>n_c=1+2r/\lambda+2\sqrt{r/\lambda}\sqrt{1+r/\lambda}$. For the diffusion limit, according to (12) and (16) the band of unstable modes is

$$k^2>k_c^2=\frac{2r}{\lambda m_0(n-1)},$$

which exists for any $n>1$. So, the diffusion limit instability condition is less restrictive than that for the dispersal instability. In Fig. 3 we plot the stability diagram for n versus r/λ. As occurs for the case of density-dependent jump rate, the dispersal instability condition depends on the quotient between the reaction rate and jump rate r/λ but for the diffusion limit it does not. All these results have also been properly checked numerically from direct integration of Eq. (4) (circles), showing again an excellent agreement with our theoretical predictions.

It is interesting to analyze alternative processes which account for population-dependent dispersal kernels. Let us consider now a Bernoulli random walk where individuals perform jumps of constant distance a but with probability $1+p(\rho)$ to jump to the right and probability $1-p(\rho)$ to jump to the left. Then, we propose

$$\Phi(z,\rho)=\tfrac{1}{2}[1+p(\rho)]\delta(z-a)+\tfrac{1}{2}[1-p(\rho)]\delta(z+a). \tag{31}$$

This clearly introduces a density-dependent bias in the random walk. Introducing (31) into (28) and considering logistic growth one finds

$$\mu=\lambda\cos(ka)-\lambda-r-i\lambda\sin(ka)[p(1)+p'(1)].$$

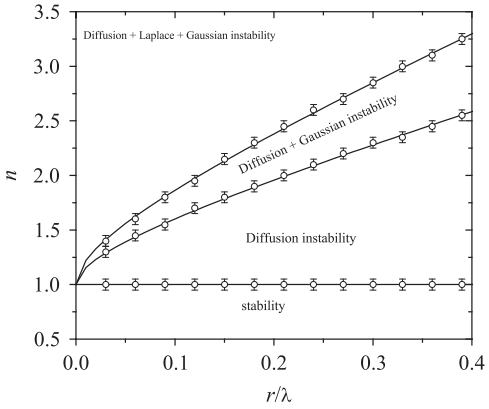

Fig. 3. Parameter space diagram for the regions of stability and instability for diffusion limit, Gaussian and Laplace kernels. Circles and the corresponding error bars correspond to the results obtained from the numerical integration of Eq. (4).

Due to the bias present in the dispersal kernel (31), the dispersion relation becomes complex and to get the instability condition we must require $\mathrm{Re}(\mu)>0$ which implies $\cos(ka)>1+r/\lambda$, which cannot be fulfilled for k real. So, there is no spatial instability in this case. Finally, let us consider the case of non-biased random walk but with a dispersal distance depending on the density. That is,

$$\Phi(z,\rho)=\tfrac{1}{2}\,\delta[z-a(\rho)]+\tfrac{1}{2}\delta[z+a(\rho)]. \tag{32}$$

From (28) and (32) the dispersal relation is

$$\mu=\lambda\{\cos[ka(1)]-ka'(1)\sin[ka(1)]\}-\lambda-r.$$

It is easy to check that in this case there exists always a band of unstable nodes, so the spatial instability is always possible in this case for any r/λ and $a(\rho)$.

5. Conclusions

Macroscopic equations for reaction–diffusion–aggregation and reaction–diffusion–advection–aggregation have been derived from general Markovian random walks where the jump rate or the dispersal kernel are density-dependent. We have provided a clear and simple microscopic interpretation for the diffusion coefficient and the advection coefficient in terms of the moments of the dispersal kernel. The diffusion limit for aggregative individuals is recovered by considering the small jump scale approximation. Since many organisms move according to dispersal kernels rather than diffusively (Kot et al., 1996), our results are ecologically relevant. It is well known that dispersal kernels modify the invasion rate of populations in comparison to the corresponding rates for diffusive evolution (Campos et al., 2006; Kot et al., 1996). Here we have shown that something similar occurs for the onset of spatial instabilities. We have obtained the sufficient conditions for the emergence of dispersal/diffusion driven spatial pattern and have determined that the critical parameter that controls the onset of instability is the ratio between the reaction and jump rates. We have compared the conditions for the emergence of spatial instabilities between reaction–diffusion–aggregation and reaction–dispersal–aggregation processes. We have found that dispersal processes has a more stabilizing effect than their diffusion counterparts. We have studied two specific situations: first, general dispersal kernels with the same mean and variance and density-dependent jump rate and second specific dispersal kernels with the same mean and density-dependent variance and constant jump rate. In the first case we have studied the specific cases of Gaussian, Laplace, Lévy and top-hat dispersal kernels, have depicted the corresponding stability diagrams and have compared to numerical simulations. An important result found is that spatial instability does not appear in reaction-dispersal-aggregation if the ratio between the characteristic reaction and jump rate exceeds a certain threshold value. This does not occur for reaction–diffusion–aggregation. In the second case we have shown that nonlinear advection also has a stabilizing effect and damps small spatio-temporal perturbation of the stable equilibrium state. In both cases we have found that the inclusion of higher moments of the dispersal kernels in the description of the transport process has also an stabilizing effect shrinking the region of instability in the space parameters in comparison with the diffusion regime. Our results show that the underlying microscopic mechanism for the population motion is critical for the emergence of spatial instabilities due to population aggregation and should be taken into account in those ecological applications where the dispersal kernel is more adequate than diffusion.

Acknowledgments

The work has been funded by Generalitat de Catalunya under Grant 2009 SGR-164 (VM and DC) and by MICINN Grant no. FIS 2006-12296-C02-01 (VM). IP acknowledges MINECO (Spain) and DURSI for financial support under Projects no. FIS 2011-22603 and no. 2009SGR-634, respectively.

References

Almeida, R.C., Delphim, S.A., da Costa, M.I.S., 2006. A numerical model to solve single-species invasion problems with Allee effects. Ecol. Model. 192, 601–617.
Armstrong, N.J., Painter, K.J., Sherratt, J.A., 2006. A continuum approach to modelling cell–cell adhesion. J. Theor. Biol. 243, 98–113.
Balasuriya, S., Gottwald, G.A., 2010. Wavespeed in reaction–diffusion systems, with applications to chemotaxis and population pressure. J. Math. Biol. 61, 377–399.
Britton, N.F., 1989. Aggregation and the competitive exclusion principle. J. Theor. Biol. 136, 57–66.
Cates, M.E., Marenduzzo, D., Pagonabarraga, I., Tailleur, J., 2010. Arrested phase separation in reproducing bacteria creates a generic route to pattern formation. Proc. Natl. Acad. Sci. 107, 11715–11720.
Campos, D., Fort, J., Méndez, V., 2006. Transport on fractal river networks. Application to migration fronts. Theor. Popul. Biol. 69, 88–93.
Clark, J.S., 1998. Why trees migrate so fast: confronting theory with dispersal biology and the paleorecord. Am. Nat. 152, 204–224.
de Jager, M., Weissing, F.J., Herman, P.M.J., Nolet, B.A., van de Koppel, J., 2011. Lévy walks evolve through interaction between movement and environmental complexity. Science 332, 1551–1553.
Fedotov, S., Moss, D., Campos, D., 2008. Stochastic model for population migration and the growth of human settlements during the Neolithic transition. Phys. Rev. E 78, 026107.
Fedotov, S., 2011. Subdiffusion, chemotaxis, and anomalous aggregation. Phys. Rev. E 83, 021110.
Grünbaum, D., Okubo, A., 1994. Modelling social animal aggregations. In: Levin, S.A. (Ed.), Frontiers of Theoretical Biology, Lecture Notes in Biomathematics, vol. 100. Springer-Verlag.
Gurney, W.S.C., Nisbet, R.M., 1975. The regulation of inhomogeneous populations. J. Theor. Biol. 52, 441–457.
Igoshin, O.A., Mogilner, A., Welch, R.D., Kaiser, D., Oster, G., 2001. Pattern formation and traveling waves in myobacteria: theory and modeling. Proc. Natl. Acad. Sci. 98, 14913–14918.
Igoshin, O.A., Welch, R., Kaiser, D., Oster, G., 2004. Waves and aggregation patterns in myobacteria. Proc. Natl. Acad. Sci. 101, 4256–4261.
Ims, R.A., Andreassen, H.P., 2005. Density-dependent dispersal and spatial population dynamics. Proc. R. Soc. B 272, 913–918.
Kenkre, V.M., Kumar, N., 2008. Nonlinearity in bacterial population dynamics: proposal for experiments for the observation of abrupt transitions in patches. Proc. Natl. Acad. Sci. 105, 18752–18757.
Kot, M., Lewis, M.A., van den Driessche, P., 1996. Dispersal data and the spread of invading organisms. Ecology 77, 2027–2042.
Maini, P.K., Malaguti, L., Marcelli, C., Matucci, S., 2006. Diffusion–aggregation processes with mono-stable reaction terms. Discrete Continuous Dyn. Syst. B 6, 1175–1189.
Matthysen, E., 2005. Density-dependent dispersal in birds and mammals. Ecography 28, 403–416.

Méndez, V., Fedotov, S., Horsthemke, W., 2010. Reaction-Transport Systems: Mesoscopic Foundations, Fronts, and Spatial Instabilities. Springer-Verlag, Berlin.
Murray, J.D., 2003. Mathematical Biology. Springer, New York.
Okubo, A., 1986. Dynamical aspects of animal grouping: swarms, schools, flocks, and herds. Adv. Biophys. 22, 1–94.
Okubo, A., Kareiva, P., 2001. Some examples of animal diffusion. In: Okubo, A., Levin, S.A. (Eds.), Diffusion and Ecological Problems: Modern Perspectives. Springer, New York, NY, USA, pp. 170–196.
Othmer, H.G., Dunbar, S.R., Alt, W., 1988. Models of dispersal in biological systems. J. Math. Biol. 26, 263–298.
Petrovskii, S.V., Li, B.-L., 2003. An exactly solvable model of population dynamics with density-dependent migrations and the Allee effect. Math. Biosci. 186, 79–91.
Sánchez-Garduño, F., Maini, P.K., Pérez-Velázquez, J., 2010. A non-linear degenerate equation for direct aggregation and traveling wave dynamics. Discrete Continuous Dyn. Sys. B 13, 455–487.
Shigesada, N., Kawasaki, K., Teramoto, E., 1979. Spatial segregation of interacting species. J. Theor. Biol. 79, 83–99.
Skellam, J.G., 1951. Random dispersal in theoretical populations. Biometrika 38, 196–218.
Smith, M.J., Sherratt, J.A., Lambin, X., 2008. The effects of density-dependent dispersal on the spatiotemporal dynamics of cyclic populations. J. Theor. Biol. 254, 264–274.
Tailleur, J., Cates, M.E., 2008. Statistical mechanics of interacting run-and-tumble bacteria. Phys. Rev. Lett. 100, 218103.
Thompson, A.G., Tailleur, J., Cates, M.E., Blythe, R.A., 2011. Lattice models of nonequilibrium bacterial dynamics. J. Stat. Mech. Theor. Exp. P02029.
Turchin, P., 1989. Population consequences of aggregative movement. J. Animal Ecol. 58, 75–100.
Veit, R.R., Lewis, M.A., 1996. Dispersal population growth and the Allee effect: dynamics of the house finch invasion of eastern North America. Am. Nat. 148, 255–274.
Wu, J.G., Vankat, J.L., Barlas, Y., 1993. Effects of patch connectivity and arrangement on animal metapopulation dynamics- a simulation study. Ecol. Model. 65, 221–254.